Int. J. Multiphase Flow Vol. 16, No. 5, pp. 789–798, 1990
Printed in Great Britain.

0301-9322/90 $3.00 + 0.00

A STUDY OF THE RAPID DEPRESSURIZATION OF HOT WATER AND THE DYNAMICS OF VAPOUR BUBBLE GENERATION IN SUPERHEATED WATER

J. BARTÁK
National Research Institute for Machine Design (SVUSS), 190 11 Prague 9, Czechoslovakia

(*Received* 13 *February* 1989; *in revised form* 6 *January* 1990)

Abstract—Liquid can be brought to a superheated state by means of very rapid depressurization. Such situations are typical for pipe rupture accidents, which can occur in processing equipment and have to be taken into account, for example, in the design of nuclear power plants with water-cooled reactors. An experimental investigation was carried out using a horizontal pipe attached to a pressure vessel. Rapid depressurization was achieved with the use of a rupture disc assembly. The paper describes the most important test results, a method for calculating the pressure undershoot below the saturation pressure and a simplified model of expansion wave propagation with vapour bubble generation in superheated liquid. On the basis of this model, the density of nucleation sites and the evolution of pressure and void fraction in the two-phase mixture can be estimated.

Key Words: depressurization, metastable states, wave propagation, bubble growth

1. INTRODUCTION

The hypothetical large break loss-of-coolant accident (LOCA) of a pressurized water nuclear reactor (PWR) is initiated by a sudden rupture of the primary coolant piping. A depressurization wave is created at the break and it propagates in both directions into the system. The pressure in this wave falls from the initial ≈ 16 MPa to a value well below the saturation pressure corresponding to the initial temperature (≈ 300°C). Thus, for a certain amount of time the coolant is in a metastable state before the nucleation process is triggered. The extremely rapid growth of vapour bubbles in the superheated coolant has an explosive character.

The phenomenon of pressure undershoot (i.e. the decrease of pressure below the corresponding saturation pressure) was observed in the now classical blowdown tests by Edwards & O'Brien (1970) and later on in other blowdown experiments as well (e.g. Rousseau & Riegel 1977; Wolfert 1976; Lienhard *et al.* 1978; Hall & Ericson 1979; Isaev & Pavlov 1980; Havelka *et al.* 1985). In these experiments, however, the main goal was the investigation of critical two-phase flows. Extensive studies of the behaviour and properties of superheated liquids and the physics of vapour bubble nucleation were carried out by Skripov and his group (Skripov 1972; Skripov *et al.* 1978, 1980, 1984; Isaev & Pavlov 1980; Bajdakov *et al.* 1983) with different liquids for a wide range of thermodynamic parameters. The tests were performed on small-scale laboratory equipment and had a rather fundamental character. Transferring the results to full-scale engineering systems with technical surfaces and technical coolants was not straightforward.

An investigation of the depressurization process directly related to the issue of LOCAs was reported by Lienhard *et al.* (1978; Alamgir *et al.* 1980; Alamgir & Lienhard 1981). The tests were carried out on 10.8 m long horizontal pipes with 12.7 and 50.8 mm i.d.s. A special method was developed for simulating the sudden pipe rupture and depressurization rates up to 200,000 MPa s^{-1} were reached. Water was used as the working liquid and thermodynamic parameters typical for a PWR were covered.

The most important conclusions derived from the investigations described above were as follows:

- Depressurization is stopped abruptly by an explosive bubble nucleation process causing, in its turn, a certain increase in pressure. After that, pressure remains almost constant for a relatively long period of time (≈ 100 ms).

- The pressure undershoot shows a strong dependence on the initial temperature of the coolant and a weaker dependence on the depressurization rate.
- The propagation velocity of the depressurization wave does not differ from the local sound velocity in the liquid.
- The purity of the liquid does not significantly affect the pressure undershoot.

The main purpose of this paper is to report on the investigation of the depressurization process in a configuration closely simulating the geometric and thermodynamic conditions of a PWR.

2. TEST FACILITY, INSTRUMENTATION AND PROCEDURE

The test facility consisted of a scaled model of the WWER-type PWR vessel and its internal structures. The model had two nozzles simulating the inlet and outlet nozzles of the primary circuit piping. To one of them a 1700 mm long, 88 mm i.d. horizontal pipe was attached. The system was heated by electrical resistance rods and pressurized using a compressed air pressurizer.

A series of 13 tests was carried out with varying initial parameters of the coolant and different diameters of the discharge diaphragm. The initial temperature of the tests varied from 130 to 300°C and the initial pressure varied from 8 to 12.5 MPa. A schematic drawing of the discharge channel is given in figure 1. Pressure and temperature gauges were located at the same cross-sections with a 200 mm distance between them. All the gauges were mounted in a horizontal plane at the level of the discharge channel axis to exclude the influence of temperature differences between the top and the bottom of the channel. Pressure transients were measured with piezoelectric transducers, for temperature measurements coated NiCr–Ni thermocouples were used. The pressure transients were recorded on a multichannel tape recorder and then digitized at lower tape speeds with a computer-based data acquisition system. The accuracy of the pressure and temperature measurements was ± 0.1 MPa and ± 0.5 K, respectively.

The sudden rupture of the pipe was simulated with using a rupture-disc assembly consisting of two rupture discs. The pressure between the discs was held equal to 50% of the pressure inside the test facility. To initiate the experiment, the pressure between the discs was rapidly raised, forcing the outer disc to break. After that, the inner disc was ruptured by the pressure inside the test section. Using this method, the depressurization rates ranged from 10,000 to 40,000 MPa s^{-1}.

3. DISCUSSION OF THE EXPERIMENTAL RESULTS

3.1. Depressurization wave propagation velocity

This velocity was evaluated from the pressure transients measured at different locations of the discharge channel. Due to the high velocity and small distance between the pressure gauges, the error of this measurement ranges from 15 to 20%. The deviation of the measured propagation velocities from the local sound velocities was never $> 18\%$. The change in the local sound velocity caused by the elasticity of the pipe wall was found to be negligible for the 10 mm thick pipe wall (this effect was "hidden" in the error bound of the measurement).

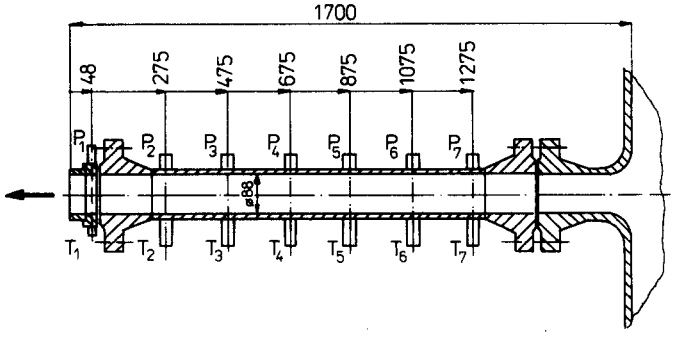

Figure 1. The horizontal experimental channel.

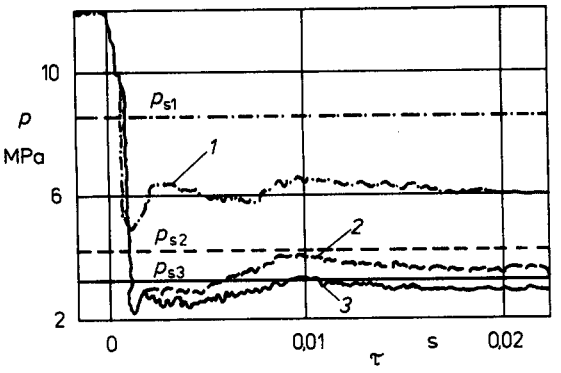

Figure 2. Pressure transients for three different initial temperatures: 1—$T = 299$°C; 2—$T = 254$°C; 3—$T = 240$°C.

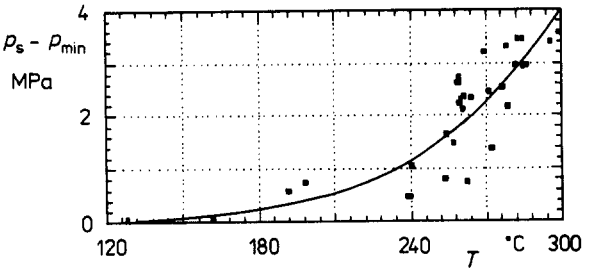

Figure 3. Pressure undershoot data.

3.2. *Amplitude of the depressurization wave*

For the analyses of the expansion wave measured at a location adjacent to the discharge cross-section a larger set of test data was available, including those from previously performed test series with short discharge channels. The amplitude $(p_0 - p_{min})$ of the wave can be divided in two parts:

$$p_0 - p_{min} = (p_0 - p_s) + (p_s - p_{min}). \quad [1]$$

Here p_0 is the initial pressure, p_s is the saturation pressure corresponding to the initial temperature and p_{min} is the minimum pressure behind the depressurization wave. The first term in [1] is given uniquely by the initial conditions of the coolant, whereas the second gives the pressure undershoot below the saturation pressure. It is this term which is in our scope of interest.

The pressure transients for three different initial temperatures are plotted in figure 2. The pressure undershoot data and a least-squares fit representing the dependence of pressure undershoot on temperature are shown in figure 3. The rather widely scattered data indicate the existence of other parameters affecting the pressure undershoot.

The initial pressure has no significant influence on the pressure undershoot, as can be seen from figure 4 where pressure transients for three different pressure levels are plotted.

The depressurization rate proved to be an important parameter. It can depend on a large variety of parameters and conditions (diameter of the discharge cross-section, material and physical properties of the rupture discs, mass of the rupture discs, initial pressure and others). As it is almost impossible to find explicit functions describing these complex dependencies, the depressurization rate was treated as an independent parameter.

3.3. *The reflected pressure wave*

The pressure transients measured in our tests begin to differ from those registered in the earlier investigations described above (in all of them a blowdown pipe with a closed end was used) from

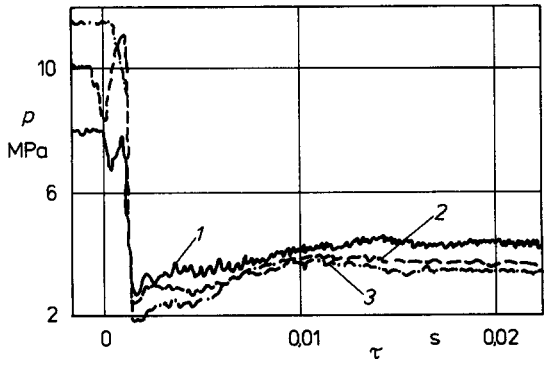

Figure 4. Pressure transients for three different initial pressures: 1—$p = 7.9$ MPa; 2—$p = 10.1$ MPa; 3—$p = 11.5$ MPa.

the moment when the reflected pressure wave reaches a given cross-section of the pipe. The depressurization wave propagates along the pipe and it is partially reflected as a pressure wave at the entrance of the pipe into the large volume of the vessel. The behaviour of the reflected wave is strongly dependent upon the thermodynamic conditions in the pipe behind the primary expansion wave. From this point of view, the tests can be divided into two groups with a qualitatively different behaviour of the reflected wave.

The "low temperature" group with initial temperatures $<220°C$ is characterized by a negligible pressure undershoot and an oscillatory high-amplitude reflected wave behind which single-phase flow conditions are resumed. The reflected wave is strongly attenuated only in the close vicinity of the discharge cross-section where a two-phase mixture persists following the onset of nucleation. The pressure transients at different locations along the pipe are shown in figure 5.

For the "high temperature" group with initial temperatures $>260°C$ (figure 6), the pressure undershoot is significant so that a non-equilibrium two-phase mixture exists behind the expansion wave along the entire discharge pipe and the reflected wave is quickly attenuated and does not have an oscillatory character in the two-phase region.

4. THEORETICAL ANALYSIS

4.1. Mechanism of nucleation in a rapid depressurization process

It is well-known that homogeneous and heterogeneous nucleation mechanisms participate in the process of vapour bubble generation. Homogeneous nucleation caused by thermodynamic fluctuations becomes predominant in the region close to the spinodal line of the liquid. In our tests the pressure undershoot was far from reaching the spinodal limit. Nevertheless, the depressurization stopped very abruptly and was followed by a short-term but rapid pressure increase. This indicates an explosion-like nucleation phenomenon characteristic for homogeneous nucleation. Alamgir & Lienhard (1981) assumed that in this case the homogeneous nucleation limit was reached on the two-dimensional surface of the pipe wall. A similar assumption was made by Skripov *et al.* (1980). They came to the conclusion that the nucleation phenomenon in a rapid depressurization

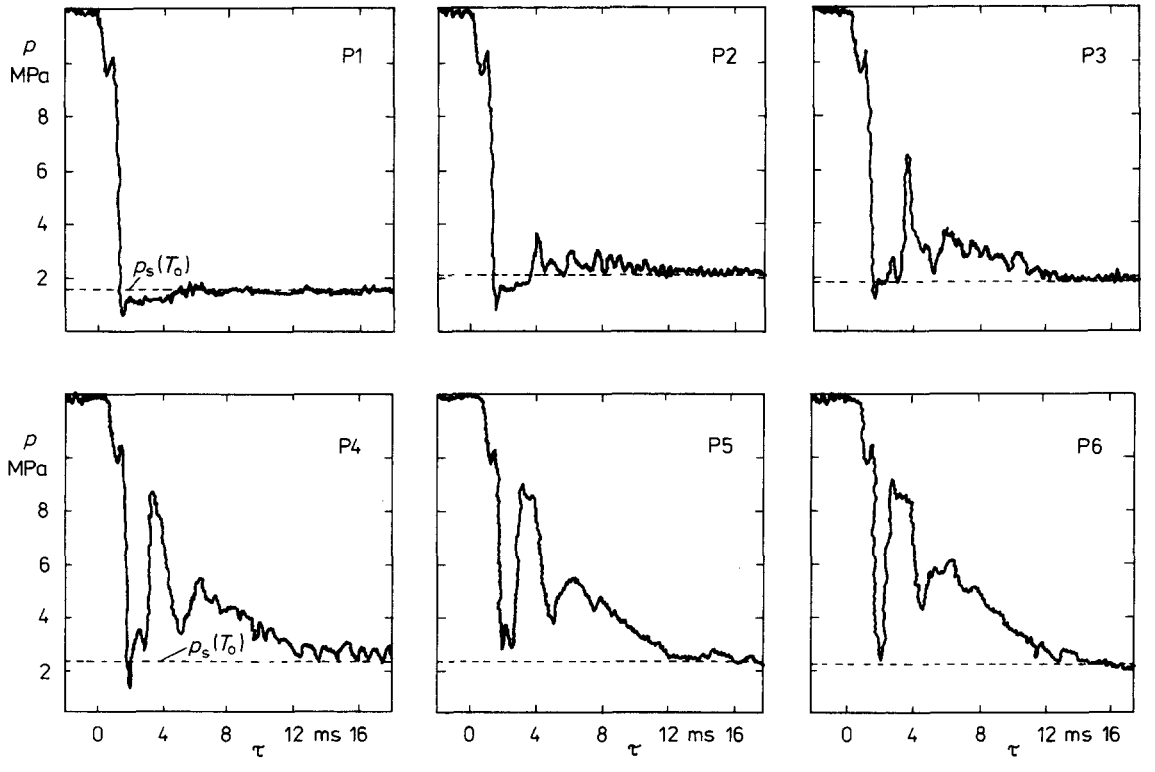

Figure 5. Pressure transients at different locations along the discharge channel for $T_0 = 220°C$.

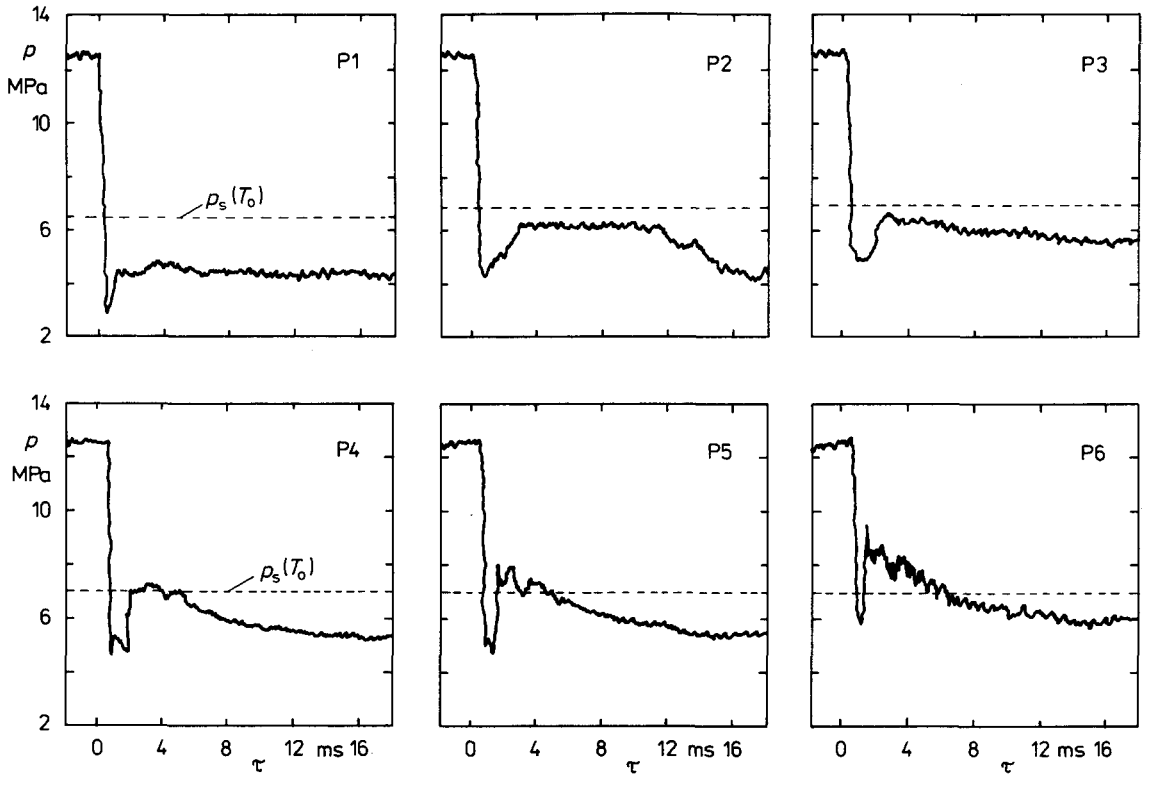

Figure 6. Pressure transients at different locations along the discharge channel for $T_0 = 290°C$.

process cannot be described by the classical "gas in a surface cavity" model but rather that it is caused by the same mechanism as homogeneous nucleation, i.e. by thermodynamic fluctuations, only with a much lower value of activation energy due to the heterogeneous origin of the nucleation sites.

The pressure transients measured in our tests indicate that such assumptions are reasonable even for large-scale equipment. This enables us to use the theory of homogeneous nucleation to describe the vapour bubble generation in a depressurization process after introducing appropriate correction factors.

4.2. Correlation for the pressure undershoot

From the theory of homogeneous nucleation (e.g. Skripov 1972; Skripov *et al.* 1980), it follows that the bubble nucleation rate J (the number of bubbles generated in a unit volume per unit time) is given by the formula

$$J = ND \exp\left(-\frac{W_c}{kT}\right), \qquad [2]$$

where N is the number of molecules in a unit volume, D is the kinetic coefficient, k is Boltzmann's constant and T is the thermodynamic temperature. The critical work W_c (the work necessary to create a bubble capable of further growth) is

$$W_c = \frac{16\pi\sigma^3}{3(p_s - p_L)^2\left(1 - \frac{v_{sL}}{v_{sG}}\right)^2}. \qquad [3]$$

Here σ is the liquid surface tension, p_s and p_L are the saturation pressure and liquid pressure, respectively, v_{sL} and v_{sG} are the liquid and vapour saturation specific volumes, respectively. For heterogeneous nucleation the critical work is much lower compared to its value for homogeneous

nucleation. To account for this, the heterogeneity factor φ was introduced in the works of Skripov (1972) and Alamgir & Lienhard (1981). The critical work will then be

$$W_c' = \varphi W_c, \qquad (\varphi < 1). \tag{4}$$

The term W_c'/kT is called the Gibbs number (Gb). From [3] and [4] it follows that

$$\mathrm{Gb} = \frac{W_c'}{kT} = \varphi \frac{W_c}{kT} = \frac{16\pi\sigma^3\varphi}{3kT(p_s - p_L)^2\left(1 - \frac{v_{sL}}{v_{sG}}\right)^2}. \tag{5}$$

From this formula the pressure undershoot can be calculated provided the values of Gb and φ are known. Alamgir & Lienhard (1981) derived their correlation for the pressure undershoot by making an assumption about the value of Gb and calculating the heterogeneity factor φ from experimental data.

To calculate the pressure undershoot the values of Gb and φ themselves are not essential. Therefore, we considered the term Gb/φ as a single unknown variable and searched for a correlation in the form

$$\frac{\mathrm{Gb}}{\varphi} = f_1(T) \cdot f_2(\Sigma). \tag{6}$$

The initial temperature T_0 and the depressurization rate Σ were found to be the most important parameters affecting the pressure undershoot. However, the influence of Σ was much smaller than the influence of T_0. For this reason the correlation for Gb/φ was developed in the form [6], where the function $f_2(\Sigma)$ played the role of a correction to the more important functional dependence $f_1(T)$. A set of more than 100 data points containing our own data and available data from Edwards & O'Brien (1970), Skripov *et al.* (1978), Lienhard *et al.* (1977) and Rassochin *et al.* (1977) was used to develop the correlation, which has the following form:

$$\log f_1(T_0) = 11 - 0.0274 T_0 \tag{7}$$

and

$$f_2(\Sigma) = 36\Sigma^{-0.37}. \tag{8}$$

In these empirical correlations, the units of T_0 and Σ are degrees Kelvin and MPa s^{-1}, respectively. The units of the numerical factors in [7] and [8] are such that they make the functions f_1 and f_2 dimensionless. The pressure undershoot is then calculated from the formula

$$p_s - p_{\min} = \left[\frac{16\pi\sigma^3}{3kT_0\left(1 - \frac{v_{sL}}{v_{sG}}\right)^2 f_1(T_0) f_2(\Sigma)}\right]^{1/2}. \tag{9}$$

All the available data are approximated by this correlation with a mean relative error of 16% (figure 7). It is valid in the temperature range from 100 to 310°C and depressurization rates from 400 to 200,000 MPa s^{-1}. The earlier correlation due to Alamgir & Lienhard (1981) approximates the same data set with a 21% mean relative error. It should be noted that it was mostly our own experimental data which were not approximated well by this earlier correlation.

Curves representing the dependence of the pressure undershoot upon temperature, based on [9], are presented in figure 8 for different values of the depressurization rate. The maximum pressure undershoot is reached for temperatures of about 320°C. For temperatures <200°C the undershoot, and hence the thermodynamic non-equilibrium of the coolant behind the expansion wave, are negligible.

4.3. The pressure and void fraction evolution behind the depressurization wave

As a reference, we shall use a slightly idealized pressure transient curve measured near the discharge cross-section and plotted in figure 9. The pressure decrease stopped at the value $p_{\min}$ and was followed by a steep pressure increase lasting for about 1 ms. The pressure then remained practically constant for a period of $\approx 10^2$ ms (the so-called quasi-static pressure). In the following theoretical considerations the reflected pressure wave is not taken into account.

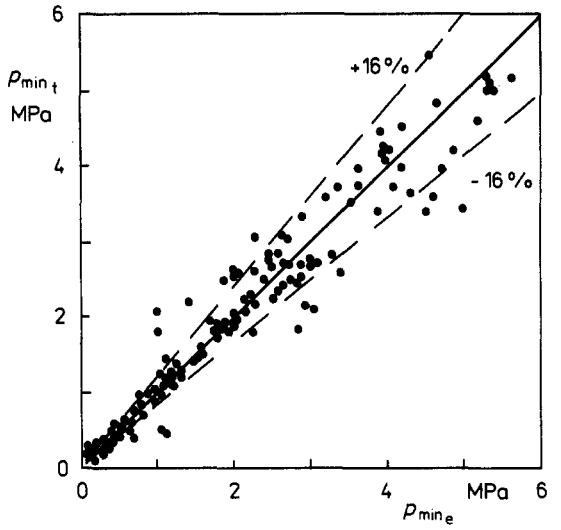

Figure 7. Comparison of the measured minimum pressure data with those predicted by [9].

For low void fractions, the density of the two-phase mixture is

$$\rho \cong \rho_L(1-\varepsilon) \qquad [10]$$

The volumetric void fraction, which is being developed during the depressurization process, can be expressed by the integral

$$\varepsilon(t,z) = \int_0^t J[p(\tau,z)] \cdot V(t-\tau)\,d\tau, \qquad [11]$$

where $V(t-\tau)$ represents the volume at time t of a bubble generated at time τ and J is the nucleation rate corresponding to the pressure p. Assuming a one-dimensional isoentropic process we introduce [10] and [11] into Euler's hydrodynamic equations:

$$\frac{\partial \rho}{\partial t} + \frac{\partial}{\partial z}(\rho w) = 0 \qquad [12]$$

and

$$\rho \frac{\partial w}{\partial t} + \rho w \frac{\partial w}{\partial z} = -\frac{\partial p}{\partial z}. \qquad [13]$$

After some algebra, we arrive at a rather complicated non-linear equation which after linearization gives

$$\frac{1}{\rho_L c_L^2}\frac{\partial^2 p}{\partial t^2} - \frac{1}{\rho_L}\frac{\partial^2 p}{\partial z^2} = \frac{\partial^2 \varepsilon}{\partial t^2}. \qquad [14]$$

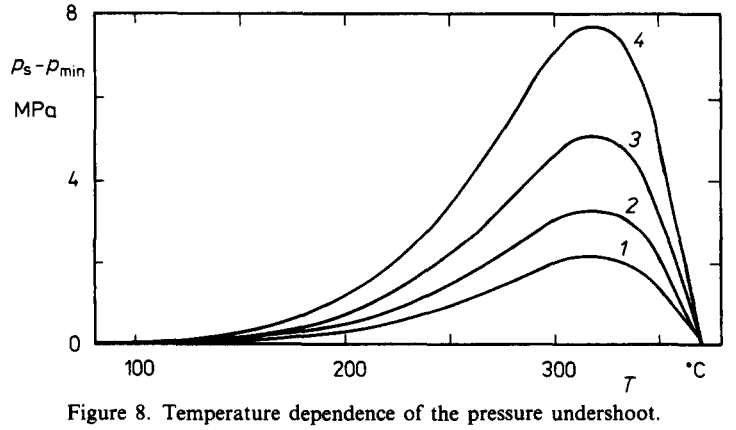

Figure 8. Temperature dependence of the pressure undershoot.

On the l.h.s. of [14] stands a wave operator and on the r.h.s. a term representing the vapour generation process. The model described was first proposed by Isaev & Pavlov (1980). We used a different method of solution for [14]—the Laplace transformation. The initial conditions are as follows:

$$p(t=0, z \geqslant 0) = p_0, \quad \frac{\partial p}{\partial t}(t=0, z \geqslant 0) = 0. \tag{15}$$

A boundary condition of the Dirichlet type is assumed at the open end of the pipe:

$$p(t \geqslant 0, z=0) = p_B(t) = \begin{cases} p_0 - \Sigma t, & t < \Delta t, \\ p_a & t \geqslant \Delta t. \end{cases} \tag{16}$$

Here p_a is the outer pressure at the open end of the pipe and Δt is the time interval which it takes to reach the pressure p_a at the open end of the pipe.

The solution of [14] has the form

$$p(t, z) = p_B\left(t - \frac{z}{c_L}\right) + \frac{\rho_L c_L z}{2} \int_0^t J\left(\tau - \frac{z}{c_L}\right) \frac{dV(t-\tau)}{dt}\, d\tau. \tag{17}$$

The nucleation rate was approximated by an exponential function.

$$J(p) = A \exp(-Bp), \tag{18}$$

where A and B are temperature functions which do not depend on the pressure. Correlations for A and B were derived from the experimental data.

To express solution [17] in an explicit form it is necessary to know the function describing the bubble volume growth in time. In general, such a function has the form

$$V(t-\tau) = b(t-\tau)^{3n}, \tag{19}$$

where the values b and n depend on the selected model of bubble growth. For the simplest models—inertial and thermal—we have $n = 1$ and $n = 1/2$, respectively. It is well-known (e.g. Jones & Zuber 1978) that in a variable pressure field the growth rate is different. For the saturation temperature changing proportionately to τ^m, the bubble radius grows proportionately to $\tau^{-m+1/2}$.

Performing several mathematical manipulations with solution [17] and using the Laplace asymptotic method (De Bruijn 1958) to estimate the integral in [17], the first approximation of the solution can be expressed as

$$p(t, z) = p_{min} + \tfrac{1}{2}\rho_L c_L z \frac{dV(t-\tau_{min})}{dt} J(p_{min}) \sqrt{\frac{\pi}{2}} \frac{1}{B\Sigma} \operatorname{erf}\left[\frac{B\Sigma(t-\tau_{min})}{\sqrt{2}}\right], \tag{20}$$

where τ_{min} denotes the time when the minimum pressure was reached at a given location, $J(p_{min})$ is the maximum nucleation rate reached when $p = p_{min}$ (i.e. $\tau = \tau_{min}$). The explicit relation for $J(p_{min})$ was found from the condition

$$\left(\frac{\partial p}{\partial \tau}\right)_{\tau = \tau_{min}} = 0. \tag{21}$$

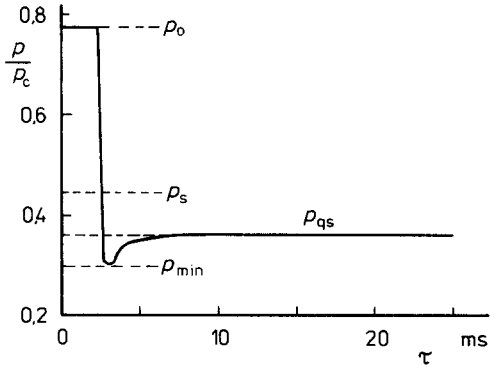

Figure 9. A typical pressure transient curve near the discharge cross-section.

The function erf in [20] reaches the value 1 very quickly, its time constant being

$$\tau_{\text{erf}} = \frac{\sqrt{2}}{B\Sigma}, \qquad [22]$$

giving a value between 0.1 and 1 ms for our tests. For $(t - \tau_{\min}) \geqslant 2\tau_{\text{erf}}$ the function $\text{erf}[B\Sigma(t - \tau_{\min})/\sqrt{2}]$ is practically equal to one. This shows that the function erf describes the rapid pressure increase after reaching the minimum, whereas further on it is only the term $\mathrm{d}V(t - \tau_{\min})/\mathrm{d}t$ that is responsible for the pressure evolution. As mentioned before, in the tests a relatively long period of pressure stabilization was observed after the initial increase (see figure 9). This corresponds to the case $\mathrm{d}V/\mathrm{d}t = \text{const}$ or $n = 0.33$ in the bubble growth model.

The asymptotic integral estimate method can also be used to find a first approximation of the volumetric void fraction from relation [11]:

$$\varepsilon(t) = \sqrt{2\pi} V(t - \tau_{\min}) J(p_{\min}) \frac{1}{B\Sigma} \text{erf}\left[\frac{B\Sigma(t - \tau_{\min})}{\sqrt{2}}\right]. \qquad [23]$$

Here again there is a short-term rapid increase in the void fraction, represented by the function $\text{erf}[B\Sigma(t - \tau_{\min})/\sqrt{2}]$, and a long-term evolution given by the bubble volume $V(t - \tau_{\min})$. With the earlier assumption of $\mathrm{d}V/\mathrm{d}t = \text{const}$ we have a linear void fraction increase. Indeed, the measured void fraction transients (e.g. Edwards & O'Brien 1970; Rohatgi *et al.* 1981/83) indicate a linear increase in void fraction after the onset of nucleation.

Equation [23] has the following structure (for $\text{erf}[B\Sigma(t - \tau_{\min})/\sqrt{2}] \to 1$):

$$\text{void fraction} = \text{const} \times \text{bubble volume}.$$

Thus, the physical meaning of the constant is the density of the nucleation sites:

$$N_{\text{nuc}} = \sqrt{2\pi} J(p_{\min}) \frac{1}{B\Sigma}. \qquad [24]$$

An analysis of this formula shows that the nucleation site density increases with temperature. In the temperature range of our tests the nucleation sites density varied from 10^9 to $10^{11}\,\text{m}^{-3}$.

5. CONCLUSIONS

The experimental results and theoretical attempts presented in this paper allow us to specify certain characteristic features of the depressurization process in a horizontal pipe attached to a pressure vessel:

(1) For initial temperatures $>240°\text{C}$ there is a significant pressure undershoot below the local saturation pressure and thus the thermodynamic non-equilibrium has to be taken into account.
(2) The rapid depressurization of hot water is stopped by explosion-like vapour generation in the superheated liquid, leading to a steep short-term increase in pressure followed by a relatively long period (from 10 to 100 ms) of quasi-static pressure. Such pressure behaviour can be disturbed by a pressure wave generated at the entrance of the pipe into the vessel. Nevertheless, unlike the pressure transients inside the pipe, the pressure transient at the discharge cross-section is almost unaffected by the reflected wave. The behaviour of the reflected wave for temperatures $<220°\text{C}$ is qualitatively different from that for temperatures $>260°\text{C}$.
(3) The nucleation of vapour bubbles in a depressurization process can be described within the framework of homogeneous nucleation theory after introducing empirical correction factors to account for the decreased activation energy of the heterogeneous nucleation sites.
(4) The initial temperature and the depressurization rate are the two most important parameters affecting the pressure undershoot.
(5) On the basis of a simplified model, the pressure and void fraction evolution consists of a short-term rapid increase due to explosive nucleation (characteristic times ranging from 0.1 to 1 ms) and a long-term evolution given by the bubble growth rate (characteristic times $\approx 10^2$ ms). Optimum agreement with measured pressure transients is achieved for the bubble volume growing linearly with time.

(6) The density of nucleation sites in a depressurization process grows with increasing temperature and ranges from 10^9 to 10^{11} m^{-3} for temperatures between 250 and 310°C.

REFERENCES

ALAMGIR, M. & LIENHARD, J. H. 1981 Correlation of pressure undershoot during hot water depressurization. *ASME Jl Heat Transfer* **103,** 52–55.

ALAMGIR, M., KAN, C. Y. & LIENHARD, J. H. 1980 An experimental study of the rapid depressurization of hot water. *ASME Jl Heat Transfer* **102,** 433–438.

ALAMGIR, M., KAN, C. Y. & LIENHARD, J. H. 1981 Early response of pressurized hot water in a pipe to a sudden break (final report). Report EPRI-NP-1867.

BAJDAKOV, V. G., MAL'CEV, S. A., POZHARSKAYA, G. I. & SKRIPOV, V. P. 1983 Vzryvnoye vskipanyie zhidkikh azota i kisloroda pri istechenyii cherez korotkie nasadki. *Teplofiz. Vys. Temp.* **21,** 959–963.

DE BRUIJN, N. G. 1958 *Asymptotic Methods in Analysis.* North-Holland, Amsterdam.

EDWARDS, A. R. & O'BRIEN, T. P. 1970 Studies of phenomena connected with the depressurization of water reactors. *J. Br. nucl. Energy Soc.* **9,** 125–135.

HALL, D. G. & ERICSON, L. 1979 The Marviken critical flow tests—a description and early results. Report INIS-mf-5057.

HAVELKA, Z., SUCHANEK, M., KODYM, O. & BARTÁK, J. 1985 Působení expanzní rázové vlny na modely vnitřních vestaveb reaktoru VVER. Report SVUSS No. 85-05014.

ISAEV, O. A. & PAVLOV, P. A. 1980 Vskipanyie zhidkosti v bol'shom ob'yeme pri bystrom sbrose davlenyia. *Teplofiz. Vys. Temp.* **18,** 812–818.

JONES, O. C. & ZUBER, N. 1978 Bubble growth in variable pressure fields. *ASME Jl Heat Transfer* **100,** 453–459.

LIENHARD, J. H., BORKAR, G. S. & TRELA, M. 1977 A rapid hot water depressurization experiment. Report NP-527, Research Project 687-1, EPRI.

LIENHARD, J. H., ALAMGIR, M. & TRELA, M. 1978 Early response of hot water to sudden release from high pressure. *ASME Jl Heat Transfer* **100,** 473–479.

RASSOCHIN, N. G., KUZEVANOV, V. S., TSIKLAURI, O. V., MARINCHEK, Z. & SELLA, G. 1977 Kriticheskyie uslovyia pri nestacionarnom istechenyii dvukhfaznoy sredy pri obryve truboprovoda. *Teplofiz. Vys. Temp.* **15,** 589–594.

ROHATGI, U. S., NEYMOTIN, L. & SAHA, P. 1981 Independent assessment of TRAC code with various blowdown experiments. Presented at the *3rd CSNI Specialists' Mtg on Transient Two-phase Flow*, Pasadena, Calif. Published in *Transient Two-phase Flow* (Edited by PLESSET, M. S., ZUBER, N. & CATTON, I.), p. 573. Hemisphere, Washington, D.C. (1983).

ROUSSEAU, J. C. & RIEGEL, B. 1977 CANON depressurization tests. Presented at the *European Two-phase Flow Gp Mtg*, Grenoble, France.

SKRIPOV, V. P. 1972 *Metastabil'naya Zhidkost'*. Nauka, Moskva.

SKRIPOV, V. P., SHURAVENKO, N. A. & ISAEV, O. A. 1978 Zapiranyie potoka v korotkikh kanalakh pri udarnom vskipanyii zhidkosti. *Teplofiz. Vys. Temp.* **16,** 563–567.

SKRIPOV, V. P., SINICYN, P. A. *et al.* 1980 *Teplofizicheskyie Svoyistva Zhidkostey v Metastabil'nom Sostoyanyii.* Atomizdat, Moskva.

SKRIPOV, V. P., ISAEV, O. A., SHURAVENKO, N. A. & KHMYL'NIN, V. A. 1984 Istechenyie vskipayushchey zhidkosti cherez korotkie nasadki pri zakriticheskom nachal'nom davlenyii. *Teplofiz. Vys. Temp.* **22,** 118–122.

WOLFERT, K. 1976 The simulation of blowdown processes with consideration of thermodynamic nonequilibrium phenomena. Presented at the *Specialists' Mtg on Transient Two-phase Flow*, Toronto, Ontario.